# Empirical effective interaction for 135 MeV nucleons

James J. Kelly
*Department of Physics and Astronomy, University of Maryland, College Park, Maryland 20742*
(Received 13 February 1989)

A model for medium modifications to the two-nucleon effective interaction, based upon the results of nuclear matter theory, is proposed for the analysis of proton inelastic scattering to normal-parity isoscalar states of self-conjugate nuclei. An empirical effective interaction is fitted to cross section and analyzing power data for the excitation by 135 MeV protons of six states of $^{16}$O simultaneously. Transition densities determined by electron scattering minimize uncertainties due to nuclear structure. Distorted waves are generated from the self-consistent optical potential computed from the same effective interaction, corrected for rearrangement effects. We find that a unique effective interaction provides a good global fit to all inelastic scattering data and is consistent with data for elastic scattering, which were not included in the fit. The density dependence of the empirical interaction is similar to, but somewhat smaller than, that of the Paris-Hamburg $G$ matrix. However, we also find that the interaction strength is reduced at zero density. These comparisons suggest effects due to nonlocal density dependence beyond the local density approximation.

## I. INTRODUCTION

The effective interaction between a projectile nucleon and a target nucleon depends strongly upon the nuclear density in the interaction region. Below about 300 MeV, the dominant source of density dependence appears to be Pauli blocking and to be amenable to treatment by nuclear matter theory. Proton inelastic scattering to normal-parity isoscalar states is quite sensitive to medium modifications of the isoscalar spin-independent central and spin-orbit components of the two-nucleon effective interaction. Furthermore, the various radial shapes of inelastic transition densities provide considerable sensitivity to the variation of the effective interaction with local density. For example, the excitation of states with transition densities peaked in the nuclear interior is sensitive to the high-density properties of the effective interaction, whereas states with surface-peaked transition densities are sensitive to the interaction at low density. In this paper, we exploit the radial specificity of inelastic scattering to deduce the parameters of a density-dependent empirical effective interaction from data for the scattering of 135-MeV protons by $^{16}$O.[1]

Several groups have recently constructed density-dependent effective interactions from solutions to a Bethe-Goldstone equation describing the propagation of an energetic nucleon in the presence of nuclear matter. Brieva, Rook, and von Geramb[2,3] (BRG) used a generalization of the Siemens[4] averaging procedure to construct an effective interaction that describes, in an average manner, Pauli correlations based upon the Hamada-Johnston[5] potential. Later, von Geramb and his Hamburg collaborators[6,7] used similar methods to construct an effective interaction [Paris-Hamburg (PH)] based upon the Paris[8] potential. Finally, Nakayama and Love[9] (NL) generalized the $G$-matrix construction of Ref. 10 to construct an effective interaction that reproduces on-shell matrix elements based upon the Bonn[11] potential. These methods and their results are reviewed in Ref. 1.

Although the medium modifications to these three effective interactions are qualitatively similar in form, their quantitative differences have a large impact upon scattering predictions. We recently compared calculations based upon all three theoretical interactions with elastic and inelastic scattering data for $^{16}$O$(p,p')$ at 135 MeV.[1] Electron scattering transition densities were used to minimize uncertainties due to nuclear structure.[12] We found that the density dependence is too strong for the BRG interaction and too weak for the NL interaction. The density dependence of the PH interaction is intermediate between these extremes and gives a good description of the data. Nevertheless, the residual discrepancies remaining in the PH interaction seem to require stronger density-dependent corrections at low density. These conclusions were found to be insensitive to reasonable variations of the approximations.

Unfortunately, existing nuclear matter calculations involve a variety of simplifications and approximations of unknown reliability. For example, we believe that differences between the methods used to reduce the nuclear matter $G$ matrix to pseudopotential form are more important to these comparisons than are differences between underlying two-nucleon potentials.[1]

Furthermore, effective interactions constructed for infinite nuclear matter are generally applied to scattering calculations for finite nuclei using some version of the local density approximation (LDA), which stipulates that the effective interaction should be the same as that for infinite nuclear matter with the density found in the interaction region. The prescription for the local density is subject to some ambiguity—reasonable choices include the density at the projectile position, the struck nucleon position, or the midpoint between these positions. Fortunately, we found that this ambiguity has little effect upon scattering calculations.[1] However, the LDA itself has not been established as an accurate approximation to

 ©1989 The American Physical Society

the $G$ matrix for finite nuclei. Nucleon orbitals are not well localized, but rather pervade the entire nucleus. Hence, even if the projectile finds a target nucleon in the low-density tail, Pauli blocking may be influenced by the penetration of the struck nucleon orbital into the high-density interior. Therefore, we might reasonably expect Pauli blocking to be enhanced for low densities and suppressed for high densities relative to LDA expectations. Nonlocal effects of this kind fall outside the purview of the LDA and may be more important than the aforementioned ambiguity in local density prescription.

Finally, we observe that extraction of neutron transition densities from proton scattering data requires a rather accurate description of the two-nucleon effective interaction and its density dependence.[13,14] We have previously demonstrated that the good intrinsic radial sensitivity of nucleon inelastic scattering for energies between about 200 and 500 MeV permits neutron transition densities to be determined even in the nuclear interior, particularly for targets with moderate $A$.[15] However, residual errors in the effective interaction may induce artificial distortion of the fitted densities and thereby limit the accuracy that can be achieved in practice. The accuracy of theoretical effective interactions presently available is not sufficient to the task.

Therefore, it is important to develop an empirical effective interaction guided by the results of nuclear matter theory. We propose a simple fitting function with 2–3 parameters for each relevant term of the effective interaction, treating real and imaginary parts separately. The functions are based upon the results of nuclear matter calculations and, with appropriate parameters, are capable of accurately reproducing any of the available calculations. The parameters are then fitted to a large body of inelastic scattering data. The data set must include cross section and analyzing power data spanning momentum transfers between about 0.5 and 2.7 $\text{fm}^{-1}$ for several normal-parity isoscalar states of a self-conjugate target. Several multipolarities and transition densities of both interior and surface character should be included to enhance the sensitivity to density dependence. The data set should be limited to relatively strong transitions for which multistep excitation is negligible. A more extensive data set may also include data for several targets or for several energies.

To be successful, the empirical effective interaction should satisfy three basic criteria. First, and foremost, the interaction must provide a good description of the data for all relevant states of a single target at a single energy. Second, the effective interaction should also be independent of target. If these criteria are satisfied, the local density approximation can be considered a sound model of the effective interaction in finite nuclei. This test of the LDA is then independent of the quantitative accuracy of nuclear matter calculations, which are presently in disarray. However, if only the first criterion is satisfied, the effective interaction may still provide a useful tool for nuclear structure applications within limited ranges of $A$ provided that the $A$ dependence is smooth. Finally, the effective interaction should depend smoothly upon projectile energy.

In this paper, we fit an empirical interaction to data for the excitation of six states of $^{16}$O by 135-MeV protons and find that a unique interaction provides an excellent description of the data for all states simultaneously. Although elastic data were not fitted, we find that the interaction fitted to inelastic scattering also describes elastic scattering well. Hence, our first criterion of success has been fulfilled. We find that substantial modifications of the free interaction persist even to zero density, but that the density dependence of the empirical interaction is somewhat weaker than predicted by nuclear matter theory. These results suggest nonlocal density dependence in finite nuclei.

Our model and calculational methods are described in Sec. II and the results are presented in Sec. III. The discussion in Sec. IV compares our approach to earlier work and describes our program for further development. Finally, our conclusions are presented in Sec. V.

## II. METHOD

### A. Linear expansion analysis

In the folding model, the scattering potential is described by the schematic "$t\rho$" form representing the convolution of an effective interaction $t$ with a transition density $\rho$. We consider only normal-parity isoscalar excitations of self-conjugate targets for which extensive electroexcitation data accurately determine the matter transition densities. Furthermore, we assume that, in the absence of significant transverse form factors, other spin and current densities are negligible. Finally, charge symmetry ensures that the neutron and proton transition densities in self-conjugate targets are very nearly equal. Therefore, electron scattering measurements specify the nuclear structure information required to interpret complementary proton scattering data and isolate the effective interaction with little residual ambiguity due to nuclear structure.

We expand the effective interaction as a linear series

$$t=\sum_n a_n t_n \tag{1}$$

so that the scattering amplitude $T=\sum_n a_n T_n$ in the distorted-wave approximation becomes

$$T_n=-\frac{\mu}{2\pi}\langle\chi_f|U_n|\chi_i\rangle\ , \tag{2}$$

where $U=\sum a_n U_n$ is the corresponding expansion of the scattering potential. We then construct the quadratic forms

$$X^{nn'}_{\alpha\beta}(\theta)=\text{Tr}[T^n(\theta)\sigma_\alpha T^{n'}(\theta)^*\sigma_\beta] \tag{3}$$

as traces over the suppressed projectile and target spin indices. The differential cross section and analyzing power finally reduce to the contractions

$$\frac{d\sigma}{d\Omega}=\frac{\mu_a\mu_b}{(2\pi)^2}\frac{k_b}{k_a}\frac{I_0(\theta)}{2j_i+1}\ , \tag{4a}$$

$$I_0(\theta)=\tfrac{1}{2}\sum_{nn'} a_n X^{nn'}_{00}(\theta)a^*_{n'}\ , \tag{4b}$$

$$I_0 D_{\alpha\beta} = \tfrac{1}{2} \sum_{nn'} a_n X^{nn'}_{\alpha\beta}(\theta) a^*_{n'} , \tag{4c}$$

where $j_i$ is the target spin and where $\mu_a$ ($\mu_b$) and $k_a$ ($k_b$) are reduced energies and projectile wave numbers in the initial (final) channel. The analyzing power $A_y = D_{y0}$ is simply an element of the depolarization matrix $D_{\alpha\beta}$. A more complete description of our method of linear expansion analysis (LEA) for direct reactions may be found in Refs. 14–19.

An efficient search procedure can now be used to fit the expansion coefficients $a_n$ to a large data set which may include several states among several targets. We begin with a good approximation to the optical potential, such as provided by the PH interaction, to generate the distorted waves $\chi$. Overlap integrals are then computed for each term $t_n$ in the linear expansion of the effective interaction. The quadratic forms are then computed and stored on disk for the entire data set. The overlap integrals and the quadratic forms are independent of the expansion coefficients $a_n$. Therefore, a very simple search algorithm can be used to optimize the coefficients. Consistency between elastic and inelastic scattering can be achieved, or at least tested, by embedding the procedure within a self-consistency cycle. The fitted interaction is used to generate new optical potentials and scattering amplitudes. The fit is then repeated. The procedure is iterated until convergence is achieved, generally within a few iterations.

### B. Reaction model

Our applications are based upon the local nonrelativistic distorted-wave approximation that was presented in Ref. 1 in considerable detail. However, note that the LEA method itself is more general and may be easily applied to nonlocal or relativistic scattering models. In this section, we merely summarize the most relevant aspects of our model; for more complete details, consult Ref. 1.

For normal-parity transitions driven by the matter density $\rho$, the scattering potential $U(r)$ seen by the incident nucleon contains only two important terms,

$$U(\mathbf{r}) = U^C(\mathbf{r}) + \nabla U^{LS}(\mathbf{r}) \otimes \frac{1}{i} \nabla \cdot \boldsymbol{\sigma} , \tag{5}$$

where

$$U^C_J(r) = \eta \frac{2}{\pi} \int dq\, q^2 j_J(qr) \tilde{t}^{\,C}(q) \tilde{\rho}_J(q) , \tag{6a}$$

$$U^{LS}_J(r) = \eta \frac{2}{\pi} \int dq\, q^2 j_J(qr) \tilde{\tau}^{\,LS}(q) \tilde{\rho}_J(q) , \tag{6b}$$

are central and spin-orbit multipole potentials, respectively. The factor $\eta$ is a Jacobian near unity.[1] The transition densities $\rho_J$ were taken directly from the electron scattering results of Ref. 12. Density dependence is included by evaluating the interaction at the projectile position. Exchange is included in the zero-range exchange approximation. The rearrangement factor $(1+\rho\partial/\partial\rho)$ is included in the inelastic interaction.[1,20] The optical potentials were also computed in the folding model using the same effective interaction that induces the transition.

### C. Effective interaction

We recently showed that the central components of all available $G$-matrix calculations could be accurately described by the simple parametrization[1]

$$\mathrm{Re}\tilde{t}^{\,C}(q,k_F) = \mathrm{Re}\tilde{t}^{\,C}(q,0) + \kappa_F^3 \left[ a_R + b_R y\left[ \frac{q}{\mu} \right] \right] , \tag{7a}$$

$$\mathrm{Im}\tilde{t}^{\,C}(q,k_F) = (1 - a_I \kappa_F^2)\mathrm{Im}\tilde{t}^{\,C}(q,0) + b_I \kappa_F^2 , \tag{7b}$$

where $\kappa_F = k_F/1.33$ describes the density relative to saturation and where $y(x) = (1+x^2)^{-1}$. The mass parameter $\mu = 3.0\ \mathrm{fm}^{-1}$ was chosen somewhat arbitrarily. The density dependence of the real part of the central interaction is described by a short-ranged repulsive core, proportional to density, representing the anticorrelation between identical nucleons. The dominant medium modification of the imaginary part of the central interaction is described by a multiplicative damping factor, linear in $\kappa_F^2$, representing Pauli blocking of the total cross section. This parametrization clearly provides greater physical insight into the properties of the effective interaction than do the voluminous tables of Yukawa coefficients supplied by the progenitors of the $G$ matrix. More importantly, this parametrization facilitates comparison between theoretical calculations and is also susceptible to phenomenological analysis.

However, we have found that this form of the empirical effective interaction is not yet adequate to our needs. The function described by Eq. (7) necessarily reduces to the free interaction $t(q,0)$ as $\kappa_F \to 0$. Although physically appealing, we have found that data for states with surface-peaked transition densities cannot be fitted unless this restriction is relaxed. Furthermore, the correlations among terms with various range parameters $\mu$ are too severe for use in this form. Finally, we require a similar model for the spin-orbit interaction. Therefore, it is necessary to generalize this model to include spin-orbit interactions and to provide the flexibility required to analyze scattering data.

Suppose that the real and imaginary parts of both the central and spin-orbit interactions are described by separate functions with the generic form

$$t_i(q,\kappa_F) = (S - a_0 \kappa_F^{\gamma_0}) t_i(q,0) + \kappa_F^{\gamma_1} \sum_{n=1}^{N} a_n q^\delta \left[ 1 + \left[ \frac{q}{\mu_n} \right]^2 \right]^{-\beta} . \tag{8}$$

If we consider the various components of the $t$ matrix to be appropriate Fourier transforms of Yukawa expansions,[1] we find that the natural exponents $\beta$ are 1 for central, 2 for spin-orbit, and 3 for tensor interactions. Similarly, we use $\delta = 2$ for tensor interactions and $\delta = 0$ otherwise. These functions can be used to reparametrize theoretical interactions by requiring the scale factors $S$ to be unity, so that the free interaction is recovered at zero density; this restriction can be relaxed in phenomenological analyses. Good fits to any of the $G$ matrices available from nuclear matter calculations are obtained using $\gamma_0 = \gamma_1 = 3$ for real parts and $\gamma_0 = \gamma_1 = 2$ for imaginary

parts of both central and spin-orbit interactions. The free interactions $t_i(q,0)$ are obtained by extrapolating the appropriate $G$ matrix to zero density.

In Figs. 1–3 we compare reparametrized 135-MeV $G$ matrices obtained by fitting the PH, NL, and BRG interactions in the ranges $0 \le q \le 3$ fm$^{-1}$ and $0.6 \le k_F \le 1.4$ fm$^{-1}$. The original theories are shown as data points and our parametrizations as solid lines. The fitted parameters are compared in Table I. In addition, the comparisons for $\mathrm{Re}t_{00}^{C}$ are clearest when presented in the low-$q$ form

$$\mathrm{Re}t^{C}(q,k_F) \approx \mathrm{Re}t^{C}(q,0) + \kappa_F^3 V_R \left[1 - \frac{q^2R^2}{6} + \cdots\right], \tag{9}$$

where $V_R$ measures the strength of the repulsive core and $R$ its range.

The excellent accuracy achieved by this analysis demonstrates that theoretical medium modifications of the effective interaction assume relatively simple forms that are qualitatively similar for all available calculations. However, the three theories differ considerably in their quantitative predictions. For $\mathrm{Re}t_{00}^{C}$, the BRG repulsive core is very strong and has a rather short range, whereas the NL core is weak and long ranged. The PH interaction is intermediate between these extremes. For $\mathrm{Im}t_{00}^{C}$, on the other hand, the BRG and NL damping factors are both substantially larger than the $a_0$ parameter for the PH interaction. The $a_1$ parameter is small for each of the $\mathrm{Im}t_{00}^{C}$ calculations. Although the three forms for $\mathrm{Re}t_0^{LS}$ differ in detail, none depends strongly on density. Finally, $\mathrm{Im}t_0^{LS}$ exhibits considerable density dependence but is rather weak.

Thus, although nuclear matter theory may describe the qualitative density dependence of the effective interaction, its quantitative predictions are presently subject to considerable ambiguity. Therefore, we seek to resolve some of these ambiguities by fitting an empirical effective interaction of similar form to data for inelastic scattering.

Unfortunately, the analysis of scattering data is complicated by correlations among the parameters. For example, the two density-dependent contributions to $\mathrm{Re}t_0^{LS}$ have similar forms for $q < 3$ fm$^{-1}$ and their coefficients tend to cancel. Similarly, it is difficult to obtain stable fits to scattering data using two independent parameters for the density dependence of either component of the central interaction. Therefore, we interpret scattering data using the simpler forms

$$\mathrm{Re}t_{00}^{C}(q,\kappa_F) = S_1 \mathrm{Re}t_{00}^{C}(q,0) + \kappa_F^3 b_1 \left[1 + \left[\frac{q}{\mu_1}\right]^2\right]^{-1}, \tag{10a}$$

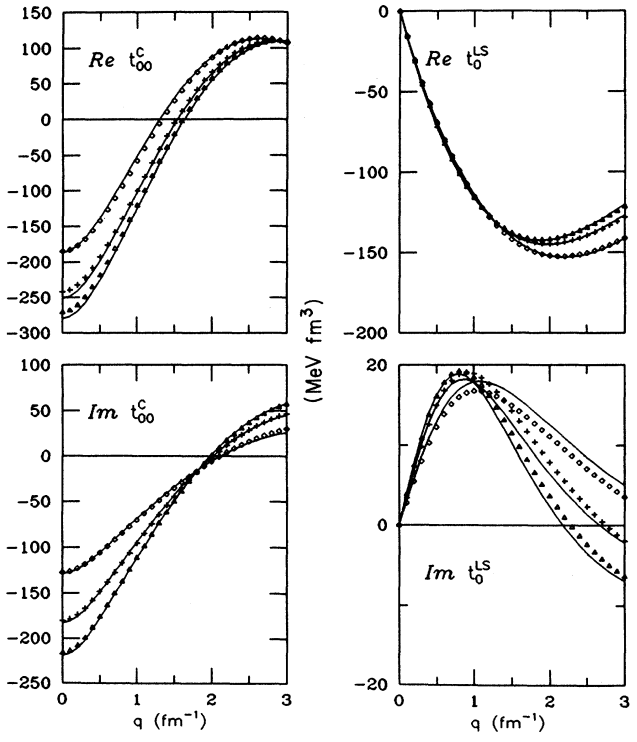


FIG. 1. Best fit to the PH effective interaction at 135 MeV. Fits to data for $k_F = 0.6$ fm$^{-1}$ (triangles), 1.0 fm$^{-1}$ (plus signs), and 1.4 fm$^{-1}$ (diamonds) are all shown as solid lines. Note that $\tilde{t}^{LS} = -k^2 \sin\theta \bar{\tau}^{LS}$ in the notation of Ref. 1.

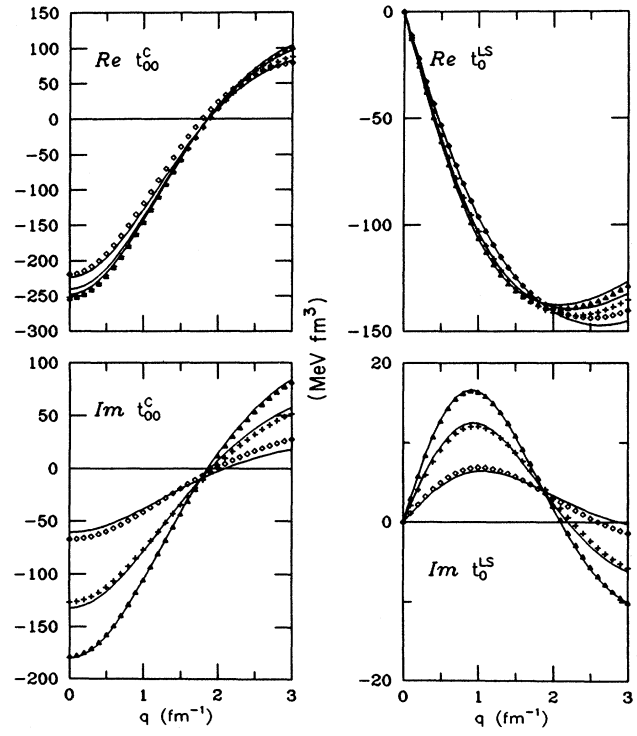


FIG. 2. Best fit to the NL effective interaction at 135 MeV. Fits to data for $k_F = 0.6$ fm$^{-1}$ (triangles), 1.0 fm$^{-1}$ (plus signs), and 1.4 fm$^{-1}$ (diamonds) are all shown as solid lines. Note that $\tilde{t}^{LS} = -k^2 \sin\theta \bar{\tau}^{LS}$ in the notation of Ref. 1.

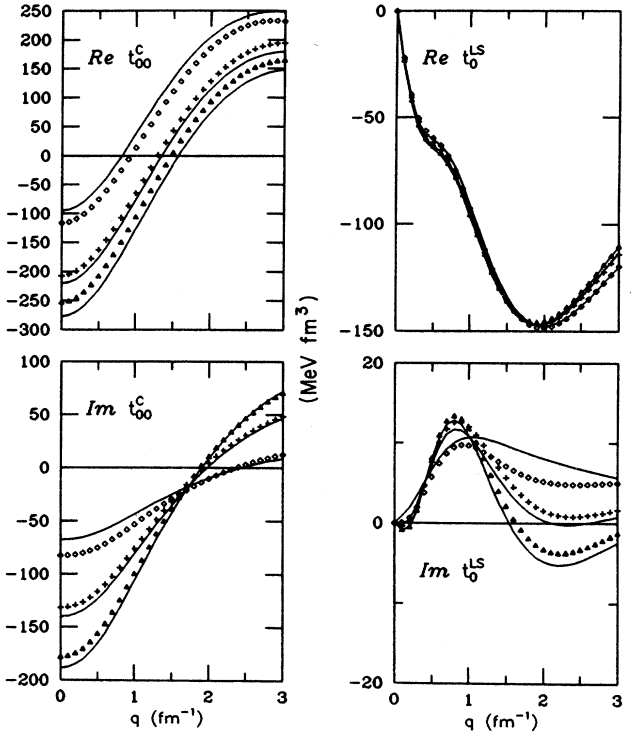


FIG. 3. Best fit to the BRG effective interaction at 135 MeV. Fits to data for $k_F=0.6$ fm$^{-1}$ (triangles), 1.0 fm$^{-1}$ (plus signs), and 1.4 fm$^{-1}$ (diamonds) are all shown as solid lines. Note that $\tilde{t}^{LS}=-k^2\sin\theta\bar{\tau}^{LS}$ in the notation of Ref. 1.

$$\mathrm{Im}t_{00}^{C}(q,\kappa_F)=(S_2-b_2\kappa_F^2)\mathrm{Im}t_{00}^{C}(q,0)\ , \tag{10b}$$

$$\mathrm{Re}\tau_0^{LS}(q,\kappa_F)=S_3\mathrm{Re}\tau_0^{LS}(q,0)+\kappa_F^3 b_3\left[1+\left[\frac{q}{\mu_3}\right]^2\right]^{-2}\ . \tag{10c}$$

Note that $b_1$ plays the role of $V_R$ and that $\mu_1$ provides a finite range comparable to $R$. We pattern the empirical effective interaction after the PH interaction, which provides the best theoretical description of normal-parity isoscalar transitions available. We find that fits nearly as good as Fig. 1 are obtained using $\mu_1=1.5$ fm$^{-1}$ and $\mu_3=6.0$ fm$^{-1}$. The corresponding coefficients are listed as "iteration 0" in Table II.

Inelastic scattering data will now be fitted using six free parameters, consisting of one scale factor $S_i$ and one density coefficient $b_i$ for the real and imaginary central components and real spin-orbit component ($i=1,3$). The $\mathrm{Im}t_0^{LS}$ component is too ineffectual to be fitted and is constrained to the PH model. The PH free interactions are used for each $t_i(q,0)$. Fortunately, we have found that the empirical interaction fitted to scattering data is relatively insensitive to the details of the parametrization.

### D. Data selection

The target $^{16}$O provides an excellent laboratory for studying medium modifications to the effective interaction. States of several multipolarities and with both interior and surface character can be resolved with only modest resolution.[12] Extensive proton scattering measurements were recently reported for two $0^+$ states, a $1^-$ state, three $2^+$ states, a $3^-$ state, and two $4^+$ states at 135 MeV.[1] From this set, we select the $0_3^+$ state at 12.049 MeV, the $1_1^-$ state at 7.117 MeV, the $2_1^+$ state at 6.917 MeV, the $2_3^+$ state at 11.521 MeV, the $3_1^-$ state at 6.130 MeV, and the $4_1^+$ state at 10.353 MeV for analysis. The data for the $4_2^+$ state are omitted because of evidence for contamination by an unresolved $3^+$ state. The $2_2^+$ state is also omitted because it is very weakly excited and shows evidence of multistep contributions.[1] The $0_2^+$ state at 6.049 MeV is difficult to resolve from the neighboring $3_1^-$ state and its data are too sparse to be worth including.

Relative weights were assigned to the data using the following criteria. First, we desired all states to have similar influence upon the analysis and for the relative weights to be independent of momentum transfer. Moreover, it is unrealistic to expect the fitted interaction to achieve $\chi_\nu^2\sim 1$ using the rather small experimental uncertainties. Second, we wanted the quality of the cross section and analyzing power fits to be similar, as measured by $\chi^2$ per datum. These criteria were satisfied by folding

TABLE I. Reparametrization of 135-MeV $G$ matrices.

| Component | Coefficient | $\mu$[a] | PH | NL | BRG |
|---|---|---|---|---|---|
| $\mathrm{Re}t_{00}^{C}$ | $a_1$ (MeV fm$^3$) | 0 | −94.71 | −62.78 | 15.60 |
| | $a_2$ (MeV fm$^3$) | 3.0 fm$^{-1}$ | 181.29 | 85.15 | 153.45 |
| | $V_R$ (MeV fm$^3$) | | 86.6 | 22.4 | 169.1 |
| | $R$ (fm) | | 1.18 | 1.59 | 0.78 |
| $\mathrm{Im}t_{00}^{C}$ | $a_0$ | | 0.443 | 0.671 | 0.674 |
| | $a_1$ (MeV fm$^3$) | 0 | −6.36 | −6.64 | −11.70 |
| $\mathrm{Re}\tau_0^{LS}$ | $a_1$ (MeV fm$^3$) | 3.0 fm$^{-1}$ | −13.80 | −18.89 | −9.90 |
| | $a_2$ (MeV fm$^3$) | 6.0 fm$^{-1}$ | 10.71 | 12.00 | 6.16 |
| $\mathrm{Im}\tau_0^{LS}$ | $a_0$ | | 0.571 | 0.728 | 0.731 |
| | $a_1$ (MeV fm$^3$) | 3.0 fm$^{-1}$ | −5.26 | −1.30 | −3.99 |

[a]An entry of 0 is to be interpreted as a delta function with $\mu^{-1}=0$.

TABLE II. Self-consistency cycle for empirical effective interaction.

| Iteration | $\chi^2_\nu$ | Re$t^C_{00}$ $S_1$ | $b_1$ | Im$t^C_{00}$ $S_2$ | $b_2$ | Re$\tau^{LS}_0$ $S_3$ | $b_3$ |
|---|---|---|---|---|---|---|---|
| 0 | 19.6 | 1.0 | 90.0 | 1.0 | 0.415 | 1.0 | 2.57 |
| 1 | 6.79 | 0.845 | 57.1 | 0.921 | 0.557 | 0.871 | 9.35 |
| 2 | 6.17 | 0.840 | 55.7 | 0.814 | 0.471 | 0.875 | 2.71 |
| 3 | 5.65 | 0.831 | 55.6 | 0.799 | 0.438 | 0.843 | 2.35 |
| 4 | 5.53 | 0.838 | 56.7 | 0.804 | 0.426 | 0.838 | 2.73 |
| 5 | 5.54 | 0.840 | 56.9 | 0.811 | 0.432 | 0.838 | 3.15 |
| 6 | 5.56 | 0.840 | 56.8 | 0.812 | 0.435 | 0.839 | 3.18 |
| Final | 5.56 | 0.839 | 56.8 | 0.812 | 0.435 | 0.840 | 3.14 |

generous additional uncertainties into the fitted data. Accordingly, we folded 5.0% relative errors into the cross-section data and folded absolute errors $\delta A_y = 0.05$ into the analyzing power data. However, we have found that the fitted interaction is actually quite insensitive to these choices. The additional errors are not included in the figures to follow.

Although the proton scattering data extend to momentum transfers as large as 3.2 fm$^{-1}$ for some states, the electron scattering data was limited to $q \leq 2.7$ fm$^{-1}$ for most states.[12] This limit corresponds to about twice the Fermi momentum, beyond which form factors tend to plummet. Moreover, several aspects of the reaction model can be expected to fail for substantially larger momentum transfer. Therefore, the range of $q$ included in the analysis was limited to 2.7 fm$^{-1}$.

Finally, we note that the $0^+_3$ state is unique in that the spin-convection density discussed in Refs. 2 and 21 may make an important contribution to the cross section near $q = 1.5$ fm$^{-1}$, where the electroexcitation form factor passes through a minimum. Hence, we have performed fits both with and without the data for this state and have obtained essentially the same fitted interaction. Although none of the fits was able to reproduce the $0^+_3$ cross section for momentum transfers between about 1.2 and 2.0 fm$^{-1}$, the analyzing power data and the remainder of the cross-section data are well fitted either way. Furthermore, the fits to the data for other states are virtually indistinguishable. Therefore, although we show calculations for the $0^+_3$ state in subsequent sections, the tabulated parameters were obtained without this data.

### E. Iteration procedure

Rearrangement contributions increase the density dependence of the effective interaction describing inelastic scattering relative to the elastic interaction. According to Cheon *et al.*,[20] the relationship between the inelastic interaction $t'$ and the elastic interaction $t$ is well approximated by

$$t' = \left[1 + \rho \frac{\partial}{\partial \rho}\right] t \ . \tag{11}$$

Although our calculations based upon the PH interaction support this relationship,[1] this result depends upon the particular theoretical $G$ matrix used. The empirical effective interaction provides an opportunity to evaluate the relationship between elastic and inelastic interactions independently of the accuracy of nuclear matter calculations.

Our fits use a self-consistency cycle. The first iteration employs distorted waves based upon an optical potential computed using the PH interaction. Six parameters of the empirical effective interaction are then fitted to the data for inelastic scattering. The initial parameters are generally chosen near those that reparametrize the PH interaction. However, indistinguishable results are obtained starting from the free interaction for the transition potentials. The fitted interaction is then used to compute a new optical potential and distorted waves. The fit is repeated and the distortion iterated until convergence is obtained. We find that good convergence is already obtained after two iterations and that true convergence is obtained within five iterations. The results we show represent the endpoint of the self-consistency cycle.

## III. RESULTS

### A. Fit to inelastic data

Fits to the inelastic scattering data are displayed in Figs. 4 and 5 as solid curves. This particular result was obtained by fitting the cross section and analyzing powers for five states simultaneously, but is essentially indistinguishable from the fit to six or even nine states. For comparison, we also show impulse approximation (IA) calculations based upon the free interaction as dotted curves and LDA calculations based upon the PH interaction as dashed curves. These latter calculations both employ PH optical potentials.

The quality of the fits is remarkable for a global optimization of data for many states. Even the rapid features in the $0^+_3$ and $1^-_1$ analyzing powers at low momentum transfer are well reproduced by these calculations based upon measured transition densities and an empirical effective interaction. The density-dependent corrections are largest for the $0^+$ and $1^-$ states, which possess transition densities with interior character. For the $0^+_3$ state,

in particular, the cross section is suppressed by nearly a factor of 10 for $q$ near 0.5 fm$^{-1}$ and the shape of the analyzing power angular distribution is also changed dramatically from the IA. These effects remain important, but are not as large, for the states with surface-peaked transition densities.

The parameters of the fitted interaction, listed in Table II, show two remarkable features. First, the scale factors applied to components of the free interaction are all in the range 0.80–0.85. Evidently, the interaction strength is substantially suppressed even for small local density. Second, the subsequent density dependence of the empirical interaction is somewhat weaker than that of the theoretical interaction, at least as represented by the PH calculation. The results suggest nonlocal density dependence in the effective interaction for finite nuclei.

The low-density suppression of the free interaction is governed primarily by the $2_1^+$ and $4_1^+$ states for which the basic LDA calculations show very little density dependence. The data for these states cannot be fitted without allowing the scale factors to vary. However, we also observe that the PH interaction seems to give slightly better results for the $3_1^-$ state than does the empirical interaction. The corrections also appear too large for the $2_3^+$ state. Evidently, the corrections required for the $2_1^+$ and $4_1^+$ states overcompensate the fits to some of the other data. These observations may reflect small inaccuracies in the local approximation to nonlocal density dependence or errors due to small multistep contributions which differ according to state. Nevertheless, such errant influences tend to be minimized in least-squares fits to large data sets including many independent transitions.

Notice that simply scaling the PH interaction is inadequate. The PH calculation falls well below the peak cross section for the $1_1^-$ state. Having reduced the interaction strength at low density for the benefit of surface states, it is then necessary to reduce the density dependence so that interior states can be fitted also. The variety of transition densities used in the analysis renders such details accessible.

Although the values of the fitted parameters depend on the choice free interaction $t(q,0)$ upon which the expansion is based, the essential characteristics do not. For example, we repeated the analysis using the Franey-Love[22] (FL) parametrization of the free $t$ matrix in place of the PH interaction at zero density. The resulting parameters are compared in Table III with our previous results. Although $\chi_\nu^2$ is somewhat worse when the fits are based upon the FL $t$ matrix, the fits to the elastic and inelastic data actually differ very little. More importantly, the two empirical effective interactions $t(q,k_F)$ are also quite similar; the differences between the two sets of parameters tend to compensate for the differences between free interactions.

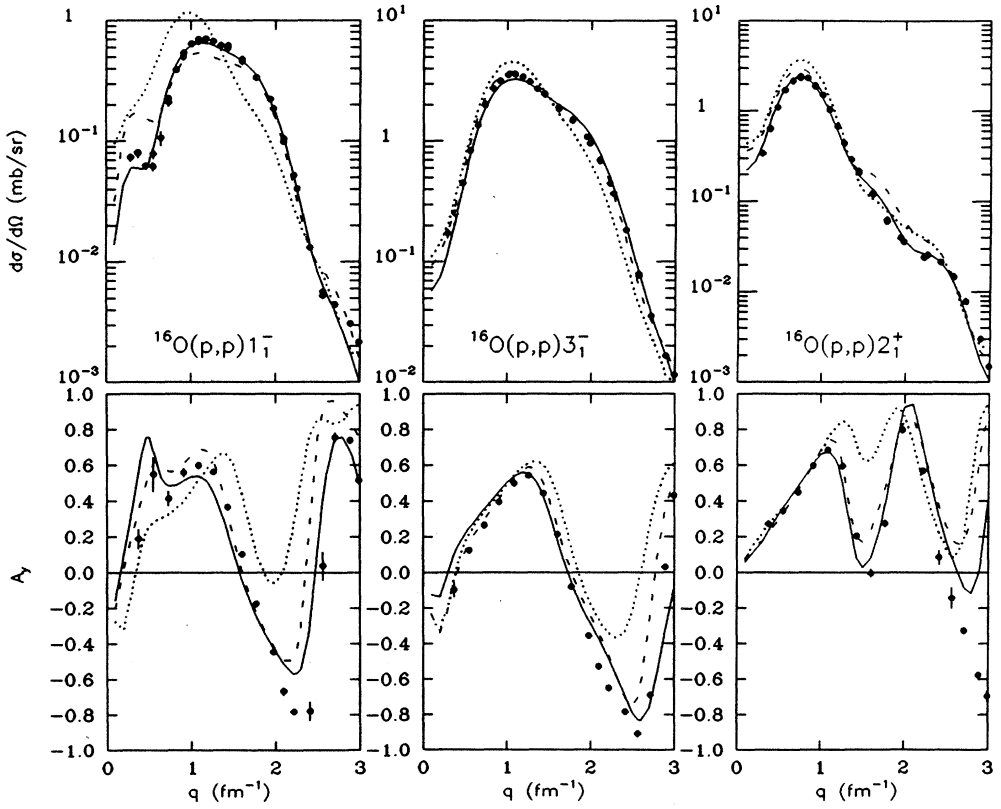


FIG. 4. Fits to the 135-MeV data for the $1_1^-$, $3_1^-$, and $2_1^+$ states of $^{16}$O are shown as solid curves. Note that only the data for $q \leq 2.7$ fm$^{-1}$ were fitted. For comparison, IA calculations are shown as dotted curves and PH calculations as dashed curves.

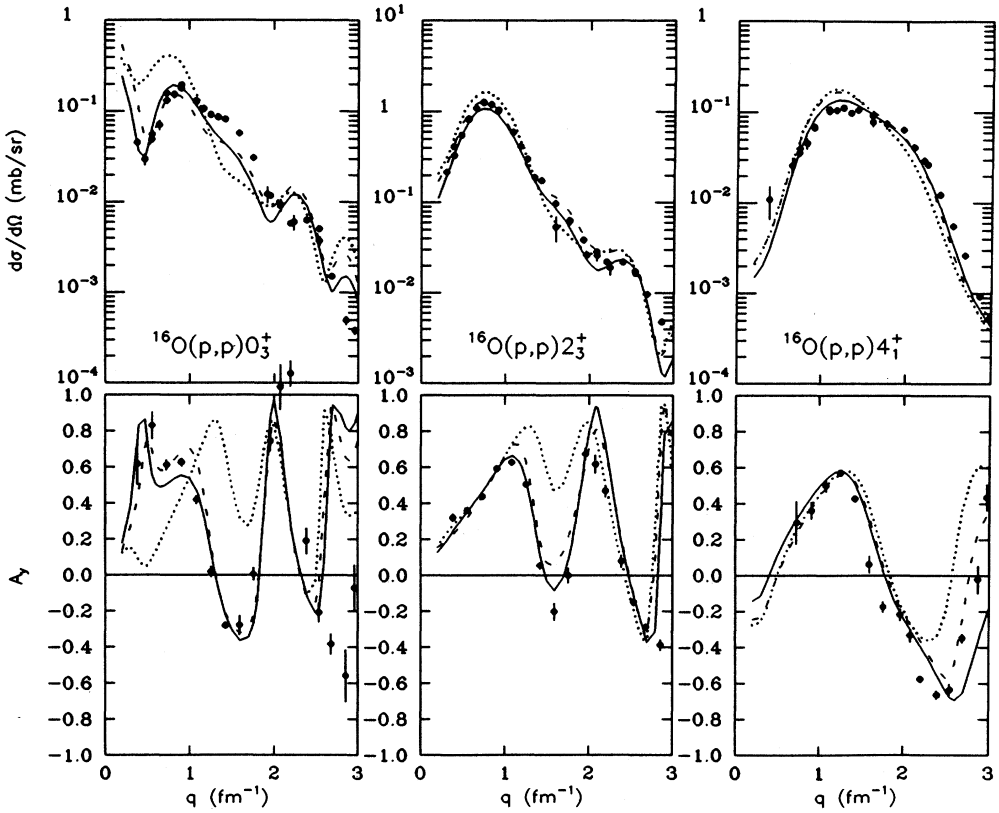


FIG. 5. Fits to the 135-MeV data for the $0_3^+$, $2_3^+$, and $4_1^+$ states of $^{16}$O are shown as solid curves. Note that only the data for $q \leq 2.7$ fm$^{-1}$ were fitted. For comparison, IA calculations are shown as dotted curves and PH calculations as dashed curves.

We also attempted to fit the data using a simpler method, motivated by the Perey effect,[23] in which all scattering potentials were multiplied by the same damping factor $[A + B(\rho/\rho_0)]$, where $\rho_0 = 0.16$ fm$^{-3}$. Ordinarily, we would expect the damping factor to be less than one in the interior (high density) and to approach unity in the surface (low density). Using five states and the PH interaction, we found $A = 0.82$ and $B = 0.33$, corresponding to an interaction which is enhanced in the interior and suppressed in the surface relative to the LDA. This result is in good qualitative agreement with the more sophisticated empirical effective interaction, but is in complete disagreement with the conventional Perey effect.

Finally, the results are essentially independent of the particular parametrization used for the empirical interaction and of the subset of states used in the analysis. Similar results were obtained in preliminary analyses using related fitting functions and as many as nine states. The relative weights assigned to cross section and analyzing powers also matter little. Similar (preliminary) results have also been obtained for $^{28}$Si and $^{40}$Ca and for several energies between 100 and 318 MeV.[24–26]

Therefore, we consider the essential features of enhanced medium modifications for low density and suppressed medium modifications for high density to be well-established features of the effective interaction for finite nuclei. Although these effects can be understood as arising from nonlocal aspects of Pauli blocking in finite systems, the fact that a unique empirical effective interaction used within the LDA provides a consistent description of the data for many states suggests that the $G$ matrix for finite nuclei is nevertheless amenable to a good local approximation.

### B. Self-consistency

The behavior of the self-consistency cycle is documented in Table II. The essential characteristics of the in-

TABLE III. Dependence upon free interaction.

| Free interaction | $\chi_\nu^2$ | Re$t_{00}^C$ $S_1$ | Re$t_{00}^C$ $b_1$ | Im$t_{00}^C$ $S_2$ | Im$t_{00}^C$ $b_2$ | Re$\tau_0^{LS}$ $S_3$ | Re$\tau_0^{LS}$ $b_3$ |
|---|---|---|---|---|---|---|---|
| PH[a] | 5.56 | 0.839 | 56.8 | 0.812 | 0.435 | 0.840 | 3.14 |
| FL[b] | 7.23 | 0.863 | 65.0 | 0.703 | 0.390 | 0.758 | 4.34 |

[a]Reference 6.
[b]Reference 22.

teraction are well established in the first iteration. Most of the parameters change very little during iteration because the distorting potential has only a relatively small effect upon the shape of the angular distribution. However, because the absorptive potential does affect the magnitude of the differential cross section directly, the parameters of the imaginary central interaction do change significantly and in a characteristic manner. The optical potentials at the beginning and the end of the self-consistency cycle are compared with the PH calculation in Fig. 6. The imaginary part of the central optical potential arising from the fitted interaction is weaker than the corresponding PH potential used in the first iteration. Hence, the amplitude of the distorted waves is increased when the fitted interaction is used to generate the distorting potential. To maintain the observed inelastic cross section, the fit then finds it necessary to reduce the interaction strength and its density dependence by decreasing $S_2$ and $b_2$ for $\mathrm{Im}t^C$. Upon iteration, the flux increase must again be compensated by similar parameter changes. About five iterations are required to damp this positive feedback. The change in $b_3$ for $\mathrm{Re}\tau^{LS}$ in the first two iterations is due to its correlation with $\mathrm{Im}t^C$ through their mutual effects upon $A_y$.

We find that the real central and spin-orbit optical potentials emerging from the fitted interaction are quite similar to those predicted by the PH theory, but that the absorptive potential is substantially reduced. Thus, although the fitted interaction is generally weaker than the PH interaction, both give similar cross sections for interior states because the increased flux partially compensates for the reduced transition potentials. In fact, the fitted peak cross section for the $1_1^-$ state is even larger than the PH theory and in better agreement with the data. Also notice that self-consistency is achieved very quickly.

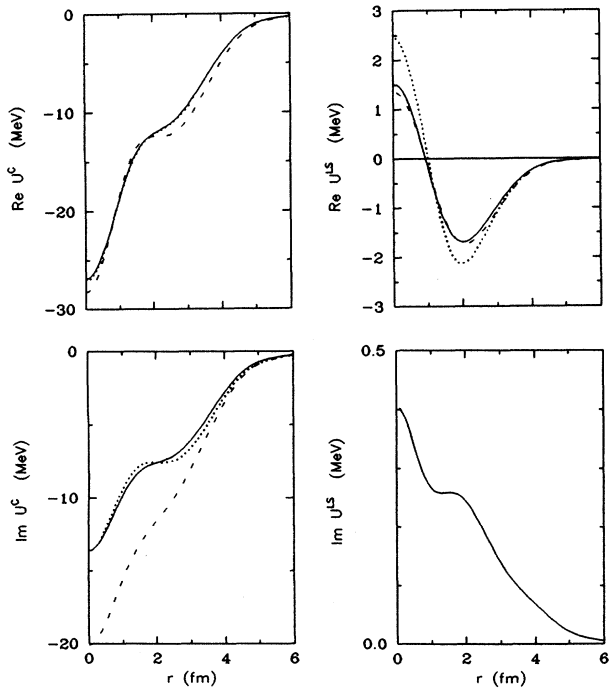


FIG. 6. Optical potentials for iteration 2 (dotted curves) and for the final fit (solid curves) are compared with the PH calculation used to begin iteration 1 (dashed curves).

The $0^+$ and $1^-$ states are particularly sensitive to the distorting potential. These transition densities display two lobes with equal areas under $r^{l+2}\rho_l$, so that delicate cancellations are required to obtain the correct cross section and the rapidly varying features observed for small momentum transfers. These features are described well throughout the iteration procedure. The fact that a good description of the $0_3^+$ data is obtained, whether or not these data are fitted, also supports the consistency of the model.

We observe that the fit quality, as measured by $\chi_\nu^2$, improves slightly during iteration. However, the detailed nature of the iteration sequence depends upon both the specific parametrization and the somewhat subjective choices for data selection and assignment of relative weights. This particular search seems to overshoot the best solution and then to recover slowly. Other choices have produced more monotonic sequences. Even the fact that improvement is obtained does depend upon the details of the parametrization. In earlier analyses in which $\mu^{-1}=0$ was used for $\mathrm{Re}t^C$, iteration increased $\chi_\nu^2$ slightly. In either case, the fact that iteration only produces small changes in the parameters and the fit supports the internal consistency of the model. Furthermore, the essential characteristics of the fitted interaction are always the same.

Although the elastic data were not included in the fit, the comparison shown in Fig. 7 between this data and elastic scattering calculations obtained from the empirical effective interaction is quite interesting. It is gratifying to observe that iteration of the distorting potential improves elastic scattering calculations based on the empirical interaction. Not surprisingly, neither approach is particularly accurate beyond 3 $\mathrm{fm}^{-1}$. Although differing in detail, we find that the overall quality of elastic scattering predictions made by empirical and theoretical interactions are equally good for $q \lesssim 2.7$ $\mathrm{fm}^{-1}$. Therefore, we conclude that the rearrangement factor proposed by Cheon *et al.*[20] for the relationship between inelastic and elastic interactions is essentially correct. Higher-order corrections and state-dependent effects appear to be small.

Finally, we note that if the scale factors are all constrained to unity, then iteration produces serious deterioration of the inelastic fits and poor results for elastic scattering. The damping of $\mathrm{Im}t^C$ becomes unreasonably large and the density dependence of $\mathrm{Re}\tau^{LS}$ reverses sign. Furthermore, cross sections for surface states are then too large and analyzing powers for interior states are quite poor. These conclusions are independent of the choice of free interaction, PH or FL, used in constructing the empirical interaction according to Eq. (10). Therefore, we conclude that the effective interaction for finite nuclei heals to the free interaction at low densities; the data require a residual suppression of the low-density interaction.

### C. Empirical interaction

The individual components of the empirical effective interaction are compared with corresponding components of the PH interaction in Fig. 8. The symbols represent the PH interaction at the four Fermi momenta $k_F=0.0$, 0.6, 1.0, and 1.4 fm$^{-1}$, corresponding roughly to zero density and a tenth, a half, and full saturation density. Solid curves are used to represent the empirical interaction for the same densities.

We find that all three components of the fitted interaction (Re$t_{00}^C$, Im$t_{00}^C$, Re$\tau_0^{LS}$) are reduced by factors of about 0.82 relative to the PH theory at low density. Furthermore, the subsequent density dependence of the empirical effective interaction is generally smaller than predicted by nuclear matter theories. The density dependence of Re$t_{00}^C$ is substantially smaller in the fit than predicted by the PH or BRG theories, but is still larger than the NL prediction. The density dependence of Im$t_{00}^C$ is similar to the PH prediction, but substantially smaller than the NL or BRG predictions. Finally, the density dependence of Re$\tau_0^{LS}$ is small and remains similar to the PH theory. Therefore, we conclude that medium modifications of the effective interaction are enhanced at low density and suppressed at high density relative to expectations based upon the local density approximation. These results are consistent with our simple expectations for the $G$ matrix in finite nuclei.

On the simplest level, the empirical interaction is approximately 0.82 times the PH interaction. In fact, we recently used a comparable scale factor to fit a neutron transition density to data for the $2_1^+$ state of $^{18}$O.[14] However, more accurate results require the full parametrization. In particular, the scale factor approach would underestimate the density dependence of Im$t^C$. Moreover, a simple scale factor does not produce consistency between elastic and inelastic scattering. The Re$U^C$ and Re$U^{LS}$ optical potentials are not significantly reduced relative to the PH potentials.

Although the empirical interaction was modeled most closely after the PH interaction, the parametrization is also capable of providing good descriptions of either the BRG or the NL interactions. The similarity between our phenomenological analysis and the PH interaction can thus be interpreted as support of that particular version of the nuclear matter theory for normal-parity isoscalar transitions in this energy regime. However, the failure of the empirical interaction to heal to the free interaction at

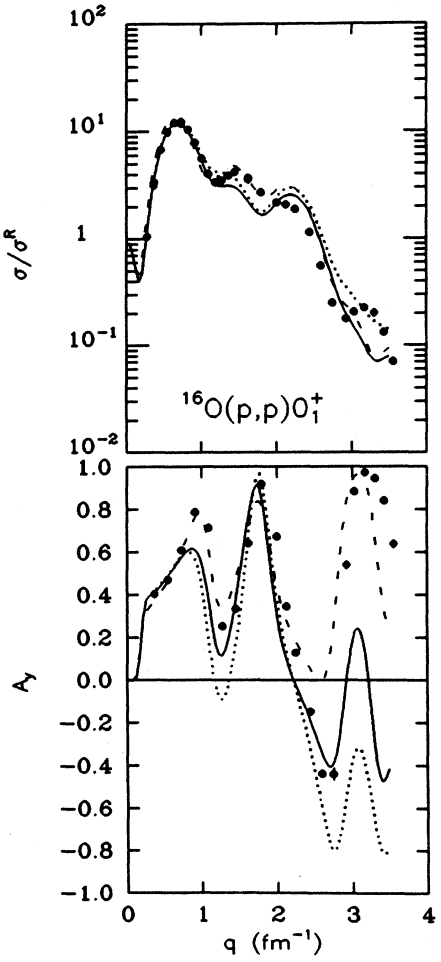


FIG. 7. Elastic scattering predictions for the first fit (dotted curves) and the final fit (solid curves) are compared with PH calculations (dashed curves) and data. Elastic cross sections are presented as ratios to Rutherford ($\sigma_R$) to enhance detail.

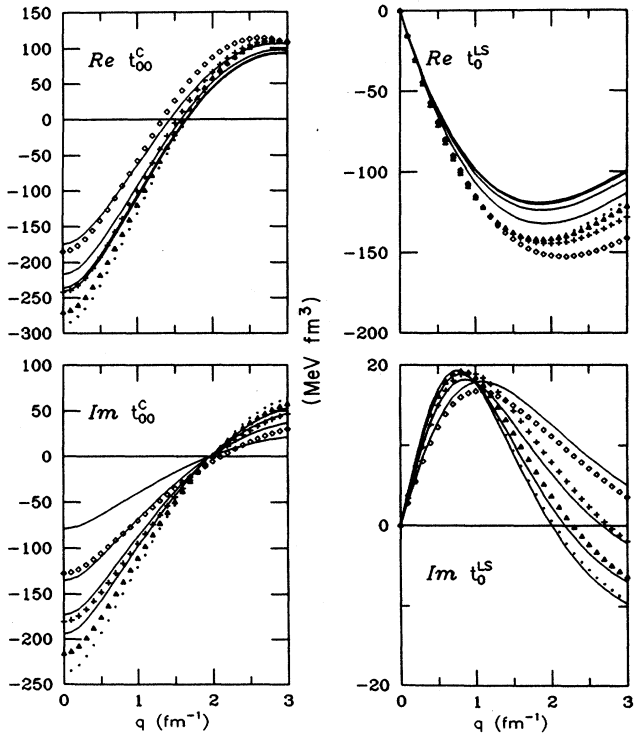


FIG. 8. The empirical effective interaction (solid curves) is compared with PH calculations for $k_F=0.0$ fm$^{-1}$ (dotted curves), 0.6 fm$^{-1}$ (triangles), 1.0 fm$^{-1}$ (plus signs), and 1.4 fm$^{-1}$ (diamonds).

zero density is strong evidence of medium modifications beyond the LDA.

## IV. DISCUSSION

For low energies, phenomenological analyses of density-dependent effects have been limited to elastic scattering. For example, Sinha has made an extensive review of these analyses of elastic scattering below 100 MeV.[27] Most of these studies employ either multiplicative damping factors or additive density-dependent cores, motivated in part by the pioneering ground-state applications of the LDA by Negele.[28] However, the consistency of these results with inelastic scattering or with modern $G$-matrix calculations has not been studied. Empirical effective interactions have also been fitted to data for elastic scattering of alphas in a single-folding model, but without the benefit of a good microscopic theory.[29]

For 200-MeV protons, Meyer *et al.*[30] have analyzed elastic scattering by $^{12}$C using a model that is similar to ours in spirit but which lacks some of the essential characteristics of the $G$ matrix. In particular, they use additive corrections proportional to the same powers of density for both real and imaginary parts, whereas $G$-matrix calculations suggest that different density-dependent corrections of the form described in Sec. II C should be invoked. Nevertheless, it is interesting to note that their fitted scale factors are similar to ours. However, we have found that their interaction fails to describe 200-MeV data for the $2_1^+$ state of $^{12}$C, especially when consistent distorted waves are used. It appears that their analysis, limited to elastic scattering by a single target, does not constrain the density-dependent parameters adequately.

Finally, Barlett *et al.*[31] have fitted a phenomenological effective interaction to 500-MeV elastic scattering data for several targets with $A \geq 40$. The effects they observe in the data are relatively small, but are consistently described by an $A$-independent interaction. However, we have found that 500-MeV elastic scattering by heavy targets is relatively insensitive to medium modifications. The much stronger effects visible in inelastic scattering seem to require medium modifications of different character.[25] Unfortunately, there exists no guidance from nuclear matter calculations for energies significantly greater than the pion production threshold.

Our approach is unique in two important respects. First, we perform a simultaneous fit to data for many transitions, thereby exploiting the radial specificity of transition densities. Hence, our analysis is more sensitive to the detailed density dependence than are fits to elastic scattering, which sample the entire nuclear volume in an average manner. Moreover, our self-consistency requirements also improve radial sensitivity through the effects of density dependence upon absorption and distortion. Second, our model is closely patterned after the results of nuclear matter theory. None of the other approaches have employed models with the full sophistication of the $G$ matrix.

We have demonstrated that a unique density-dependent effective interaction is capable of describing all relevant normal-parity isoscalar transitions in $^{16}$O excited by 135-MeV protons. The consistency of this interaction for many states, including elastic scattering, strongly suggests that the effective interaction depends strongly upon local density but not upon final state. In this sense, the empirical effective interaction provides a partial verification of the local density approximation that is independent of the predictive power of nuclear matter theory.

A more conclusive verification of the LDA requires demonstrating that the empirical effective interaction is also independent of target. To perform such a test, we need high quality data for other self-conjugate targets, including states with interior transition densities. However, such data do not exist near this energy. The only other proton scattering data for self-conjugate targets and energies near 135 MeV are limited to a few collective states with surface-peaked densities; data of this type are not very sensitive to details of the effective interaction and do not comprise an adequate data set.

We have performed experiments for $^{16}$O and for $^{40}$Ca, the heaviest self-conjugate target, at several energies between 100 and 500 MeV, taking care to observe interior densities with adequate precision.[25,26] The analysis of these data is nearing completion. This data set will provide the basis for a systematic survey of medium modifications to the two-nucleon effective interaction. In addition, we plan to extend the analysis to include elastic scattering data and to test the relationship between elastic and inelastic interactions more directly. Finally, we note that ambiguities among contributions to the effective interaction can probably be reduced by adding depolarization data to the analysis.

## V. CONCLUSIONS

The complementarity between electromagnetic and hadronic reactions provides a powerful probe of both nuclear structure and of medium modifications to effective interactions. The analysis of electroexcitation data yields precise and accurate charge and current densities which severely challenge microscopic theories of nuclear structure. These densities can also be used to constrain the nuclear structure information required to interpret complementary hadron scattering data. When the necessary structure is completely specified by electron scattering data, the medium modifications of the effective interaction for hadron scattering can be determined with little residual uncertainty due to nuclear structure. The empirical effective interaction can then be used to unfold the nuclear structure content from hadronic data for other transitions. These methods are now making radial neutron transition densities accessible to measurement and promise to stimulate new investigations into nuclear structure.

We have developed a simple parametrization of the effective interaction that accurately reproduces the results of nuclear matter theory. This model clarifies the physical content of and facilitates comparisons between theoretical calculations. More importantly, the model makes possible phenomenological analysis of medium modifications to the effective interaction. Electron

scattering measurements of transition densities for self-conjugate targets are used to minimize structure uncertainties and to isolate the effective interaction. A simultaneous fit to data for states with both interior and surface densities exploits the radial specificity of inelastic transition densities to enhance sensitivity to the detailed density dependence of the interaction. Iteration of the distorting potential arising from this same effective interaction tests the internal consistency of the model.

We have found that a unique effective interaction provides an excellent simultaneous fit to cross section and analyzing power data for the excitation of six states of $^{16}$O by 135-MeV protons. A consistent description of elastic scattering and of the distorting potential is also obtained without including elastic data in the fit. Therefore, the effective interaction depends primarily upon the local density in the interaction region, but appears to be independent of state. This result supports the hypothesis of the LDA independently of the quantitative accuracy of present nuclear matter calculations.

Although qualitatively similar to the Paris-Hamburg theory (PH), the empirical effective interaction differs in two important respects. First, the low-density limit of the effective interaction is damped with respect to the free interaction by a factor of about 0.82. Second, the subsequent dependence upon density is somewhat reduced with respect to the PH $G$ matrix, especially for $\mathrm{Re}t^C$. These properties of the empirical interaction are essentially independent of the details of the model and the fitting procedure.

Our results can be interpreted as evidence of nonlocal density-dependent effects in finite nuclei that are amenable to an accurate local approximation. It appears that Pauli blocking in regions of low density is enhanced by the penetration of nucleon orbitals into regions of higher density. Similarly, the presence of lower densities nearby seems to reduce the effectiveness of Pauli blocking in the interior. It remains to be seen how strongly these effects might depend upon target mass.

Alternatively, the fitted interaction may reflect the influence of other effects that are not described by its prototype, such as the virtual pairs predicted by relativistic theories. The success of our phenomenology suggests that it should be both possible and profitable to represent such effects in LDA form.

Therefore, the empirical effective interaction, guided by the results of nuclear matter theory, represents a promising new phenomenological method for the systematic interpretation of nucleon scattering data. For this approach to realize its full potential, the task of experiment is to acquire high-quality data over a broad energy range for many states of several self-conjugate targets. Particular attention must be paid to states with interior transition densities, which are generally weaker than the surface-peaked collective excitations. Similarly, the task of theory is to account for the fitted parameters and to elucidate the relationship between effective interactions for finite and infinite nuclei.

This work was supported by Grant No. PHY86-15512 from the National Science Foundation.

[1]J. J. Kelly, W. Bertozzi, T. N. Buti, J. M. Finn, F. W. Hersman, C. Hyde-Wright, M. V. Hynes, M. A. Kovash, B. Mudock, B. E. Norum, B. Pugh, F. N. Rad, A. D. Bacher, G. T. Emery, C. C. Foster, W. P. Jones, D. W. Miller, B. L. Berman, W. G. Love, J. A. Carr, and F. Petrovich, Phys. Rev. C **39**, 1222 (1989).

[2]F. A. Brieva and J. R. Rook, Nucl. Phys. **A291**, 299 (1977); **A291**, 317 (1977); **A297**, 206 (1978); **A307**, 493 (1978).

[3]H. V. von Geramb, F. A. Brieva, and J. R. Rook, in *Microscopic Optical Potentials,* edited by H. V. von Geramb (Springer-Verlag, Berlin, 1979), p. 104.

[4]P. J. Siemens, Nucl. Phys. **A141**, 225 (1970).

[5]T. Hamada and D. Johnston, Nucl. Phys. **34**, 382 (1962).

[6]H. V. von Geramb, in *The Interaction Between Medium Energy Nucleons in Nuclei (Indiana Cyclotron Facility, Bloomington, Indiana, 1982),* Proceedings of the Workshop on the Interactions Between Medium Energy Nucleons in Nuclei, AIP Conf. Proc. No. 97, edited by Hans-Otto Meyer (AIP, New York, 1983), p. 44.

[7]L. Rikus, K. Nakano, and H. V. von Geramb, Nucl. Phys. **A414**, 413 (1984).

[8]M. Lacombe, B. Loiseau, J. M. Richard, R. Vinh Mau, J. Cote, P. Pires, and R. de Tourreil, Phys. Rev. C **21**, 861 (1980).

[9]K. Nakayama and W. G. Love, Phys. Rev. C **38**, 51 (1988).

[10]K. Nakayama, S. Krewald, J. Speth, and W. G. Love, Nucl. Phys. **A413**, 419 (1984).

[11]R. Machleidt, K. Holinde, and Ch. Elster, Phys. Rep. **149**, 1 (1987).

[12]T. N. Buti, J. Kelly, W. Bertozzi, J. M. Finn, F. W. Hersman, C. Hyde-Wright, M. V. Hynes, M. A. Kovash, S. Kowalski, R. W. Lourie, B. Murdock, B. E. Norum , B. Pugh, C. P. Sargent, W. Turchinetz, and B. L. Berman, Phys. Rev. C **33**, 755 (1986).

[13]J. J. Kelly, in *Nuclear Structure at High Spin, Excitation, and Momentum Transfer (McCormick's Creek State Park, Bloomington, Indiana, 1985),* Proceedings of the Workshop on Nuclear Structure at High Spin, Excitation, and Momentum Transfer, AIP Conf. Proc. No. 142, edited by Hermann Nann (AIP, New York, 1986), p. 27.

[14]J. J. Kelly, W. Bertozzi, T. N. Buti, J. M. Finn, F. W. Hersman, M. V. Hynes, C. Hyde-Wright, B. E. Norum, A. D. Bacher, G. T. Emery, C. C. Foster, W. P. Jones, D. W. Miller, B. L. Berman, J. A. Carr, and F. Petrovich, Phys. Lett. **169B**, 157 (1986).

[15]J. J. Kelly, Phys. Rev. C **37**, 520 (1988).

[16]J. A. Carr, F. Petrovich, and J. Kelly, in *Neutron-Nucleus Collisions—A Probe of Nuclear Structure (Burr Oak State Park, Glouster, Ohio, 1984),* Proceedings of the Conference on Neutron-Nucleus Collisions—A Probe of Nuclear Structure, AIP Conf. Proc. No. 124, edited by J. Rapaport, R. W. Finlay, S. M. Grimes, and F. S. Dietrich (AIP, New York, 1985), p. 230.

[17]J. J. Kelly, in *Advanced Methods in the Evaluation of Nuclear Scattering Data,* Vol. 236 of *Lecture Notes in Physics,* edited

by H. J. Krappe and R. Lipperheide (Springer-Verlag, Berlin, 1985), p. 335.
[18]J. J. Kelly, in *Current Problems in Nuclear Physics,* edited by T. Paradellis and S. Kossionides (Hellenic Physical Society Conference, Athens, 1986), Vol. 1, p. 325.
[19]J. J. Kelly, in *Relations Between Structure and Reactions in Nuclear Physics,* edited by D. H. Feng, M. Vallieres, and B. H. Wildenthal (World Scientific, Singapore, 1987), p. 222.
[20]T. Cheon, K. Takayanagi, and K. Yazaki, Nucl. Phys. **A437**, 301 (1985); **A445**, 227 (1985); T. Cheon and K. Takayanagi, *ibid.* **A455**, 653 (1986).
[21]F. Petrovich, J. A. Carr, R. J. Philpott, A. W. Carpenter, and J. Kelly, Phys. Lett. **165B**, 19 (1985).
[22]M. A. Franey and W. G. Love, Phys. Rev. C **31**, 488 (1985).
[23]F. Perey and B. Buck, Nucl. Phys. **32**, 353 (1962).
[24]Q. Chen, P. P. Singh, M. C. Radhakrishna, W. P. Jones, H. Nann, and J. J. Kelly, Bull. Am. Phys. Soc. **33**, 962 (1988).
[25]J. J. Kelly, Bull. Am. Phys. Soc. **32**, 1120 (1987); A. E. Feldman, P. Boberg, B. S. Flanders, S. D. Hyman, J. J. Kelly, M. A. Khandaker, H. Seifert, P. Karen, B. E. Norum, A. Saha, and S. Nanda, *ibid.* **33**, 1570 (1988).
[26]H. Seifert, A. E. Feldman, B. S. Flanders, J. J. Kelly, M. Khandaker, Q. Chen, P. Karen, B. E. Norum, P. Welch, and A. Scott, Bull. Am. Phys. Soc. **33**, 1570 (1988).
[27]B. Sinha, Phys. Rep. **20**, 1 (1975).
[28]J. W. Negele, Phys. Rev. C **1**, 1260 (1970); J. W. Negele and D. Vautherin, *ibid.* **5**, 1472 (1972).
[29]H. J. Gils, Z. Phys. A **317**, 65 (1984).
[30]H. O. Meyer, P. Schwandt, G. L. Moake, and P. P. Singh, Phys. Rev. C **23**, 616 (1981).
[31]M. L. Barlett, W. R. Coker, G. W. Hoffman, and L. Ray, Phys. Rev. C **29**, 1407 (1984).